POLISH MARITIME RESEARCH 2 (122) 2024 Vol. 31; pp. 20-28
10.2478/pomr-2024-0018

Simulation Tests of a Drive Shaft and Propeller Control Subsystem for a Fast Boat

Andrzej Grządziela
Stanisław Hożyń *
Polish Naval Academy, Gdynia, Poland

* Corresponding author: *sunhanbing@hrbeu.edu.cn (S. Hożyń)*

ABSTRACT

This paper presents an analysis of the acceleration of a fast boat using a simulation model. Mathematical equations of ship motion dynamics with two types of propeller capabilities are developed using MATLAB and Simulink as simulation tools. The equations are extended to include the acting thrust, resistance, propeller's performance curves, and the PID governor curve for the acceleration manoeuvre. The application models the dynamic differential equations representing the vessel dynamics in one degree of freedom. MATLAB code was used to develop the ship acceleration as a multibody system. Modules of hydrodynamic forces, resistance, moments, and propeller performances were implemented to simulate the ship manoeuvring process. A comparison of the results for the boat's propulsion performance with two different propellers and the characteristics of the PID governor, which controls the fuel dose in the gas turbines, was carried out. We present a summary including a comparative analysis of the results for the boat dynamics with and without the PID governor. The results obtained here confirm significant discrepancies between the results of numerical simulations with and without the PID governor.

Keywords: simulation model, ship dynamics, acceleration, PID governor

INTRODUCTION

Estimating the acceleration of a ship can allow us to understand the vessel's behaviour during sea trials at an early stage, which can affect safety at sea and reduce the costs of sea trials. A literature analysis indicates that increasingly complex ship motion models are being used. In recent publications, analyses of ship dynamics have involved a knowledge of the propeller characteristics, the available engine torque and the couplings between wave, pitch, yaw and roll. Typically, models with four degrees of freedom (DOF), as presented by Abkowitz, Chislett and Stom-Tejsen, are introduced to describe the more advanced dynamics of the ship [1], [2]. Källström et al. developed a model using tests of a free sailing model to calibrate the heaving parameters [3]. Perez-Blanke proposed models based on the results of 4DOF experiments, which made it possible to test models with full dynamic interaction between roll, sway, yaw and wave movements[4]. Benedict and Kirchhoff presented a didactic model that described the dynamics model in a step by step manner, starting with 1DOF (surge) and ending with manoeuvring simulations [20]. Most authors have focused on the dynamics problems related to the disturbances arising from rudder forces, waves or heels[3], [5], [6], and it is challenging to find works that consider the issues of the available engine torque, rotational speed governor and propeller performance. This work focuses on a simple 1DOF model. The limitations include the performance of the gas turbine engine and the operation of the rotational speed controller, which is this paper's original goal.

In this work, we adopt similar assumptions for the run-up manoeuvre as described by Tvakoli et al. [7]. The primary task of the simulation model is to present an analysis of the results of the use of a PID governor model and a simplified model with linear acceleration characteristics for the main drive motor [8]. A comparative analysis is also conducted in which two different propellers are used to drive the boat: a four-propeller and a five-propeller. The model adopts three main simplifications: constant values for the deduction and wake coefficients, and the omission of air drag [21]. The computational method published by Marwood et al. is used to predict hull resistance [7], [9].

In order to simulate the engine's performance, a mathematical model of the brake power and torque generated is proposed in the form of interpolation curves computed from engine performance diagrams [10].

The main limitation is the curve of available torque versus rotational speed for the power turbine (PT) of the gas turbine main engine (GTE). To simulate the acceleration of the vessel, it is necessary to couple the dynamics of the propeller, the engine (including the speed governor), and the hull's resistance. For low velocities and small displacement hulls, acceleration modelling involves finding the resistance as a function of the ship's speed, which is a typical computational task. Finding the resistance of a semi-slip unit where the wetted surface area changes as a function of the speed and the angle of inclination of the propeller shafts poses more problems. Such an estimate can be made where the ship's performance in calm water is constant. When calculating the resistance of semi-planing hulls, the problem involves determining the share of components in the speed function. For fast-planing hulls, other phenomena may arise, such as resistance to water splashes, while the resistance to wave formation disappears [11]. Advances in numerical methods, such as finite volume and boundary element methods, make it possible for the hull resistance to be determined with reliable accuracy [12]. Numerical methods such as computational fluid dynamics (CFD) are now widely used to solve for the viscous flows of water and air around a vessel moving at high speeds [13]. The use of CFD methods requires a knowledge of the numerical geometry of the hull and superstructure, which may prove challenging in the preliminary stages of research. Hence, empirical and statistical methods such as those developed by Holtrop and van Oortmerssen are commonly used and valuable [14]. The key feature of these methods is that they can be easily developed and quickly put into operation, meaning that they can be used early in the design process to give an understanding of the ship's behaviour[15], [16].

When modelling a ship's speed and path changes under specific controlled conditions and simulating its motion over time, the equation of motion needs to be expressed and solved at each stage of the real-time simulation. The equation of motion for ship acceleration is usually expressed in three or four DOF. In the case of the simplifications adopted here, where only the acceleration of the ship's centre of gravity is observed, the coupling of drag and thrust forces can be analysed as a 3DOF system (surge, sway and yaw). To solve the equation of motion, the hydrodynamic forces, propulsion, added mass, gravity and buoyancy forces are analysed at each time step. In this simulation, the rudder and constant hydrodynamic forces are measured experimentally at a fixed heading, pre-calculated or measured, and then mathematically modelled. The propulsive forces are estimated using empirical formulae based on the ship's geometry, and the coefficients for the added masses are obtained either from boundary integral equations or by approximate methods [17]. It should be noted that the literature does not contain an analysis of hull dynamics in relation to the characteristics of the engine's governor.

MATLAB software is used for numerical simulations of the ship's acceleration in real time, based on the assumption that the propeller shaft drives have known PID governor characteristics. Such an assumption can always be verified under actual conditions.

The model adopted here can predict and assess a ship's performance, and can easily be adapted to specific configurations of the propellers used in this study. In this work, some geometric features of the ship parameters are omitted. The PID governor model adopted here allows for flexible adaptation to other ship propulsion engines with known parameters.

SHIP DYNAMICS

The equations describing the dynamics of a ship are well known from Newton's laws of linear and angular momentum, and are often used in numerical simulations [1], [2], [4], [5], [18], [19]. When deriving the equations, the main difficulty involves describing the hydrodynamic forces acting on the hull. Forces are generally complex functions of the ship's motion, i.e. the history of the velocity, angular velocity and rudder movement over time, and also depend on the trim and draft.

A ship is a rigid body with 6DOF, corresponding to translation in three directions and rotation around three axes. The equations of motion are conveniently expressed in terms of a coordinate system attached to the ship, and the hydrodynamic forces can be determined in this coordinate system using the symmetry of the hull. For the preliminary simulation tests, the purpose of which is to approximate the dynamics and trajectory of the boat movement, it is sufficient to use the 3DOF model shown in Fig. 1 [9].

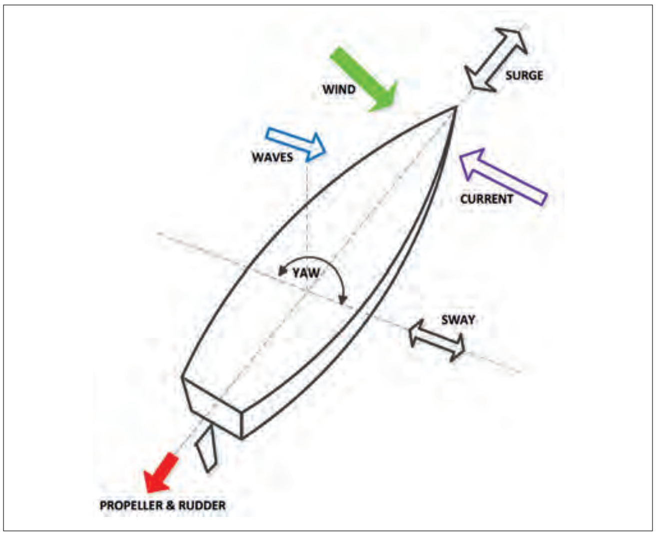

Fig. 1. 3DOF motion model of a sea-going boat with acting forces and moments

Changes in position, course and speed give rise to the ship's reaction to these forces and moments. The parameters of the changes in the inertial system are measured by internal sensors, while wind sensors and parameters of waves and drift record the readings of reference systems. The 3DOF simulation model seeks to obtain couplings between yaw, sway and surge. Data from simulation modelling can significantly improve and accelerate the design process concerning fast boat propulsion, the selection of the technical parameters of rudders, and preparation for the SAT (Sea Acceptance Tests) schedule.

The coordinate system and the definition of the basic parameters for 3DOF movement are shown in Fig. 2. The course dynamics of a fast boat can be described and simulated using Newton's equations of motion. The basic equations in the horizontal plane are first considered in a coordinate system where the origin of the axes is fixed in relation to the seabed, and secondly in a movable system, which is fixed to the boat's centre of gravity.

The path describes the trajectory of the boat's centre of gravity. In this case, the direction refers to the yaw angle of the ship's longitudinal axis relative to one of the fixed axes. The difference between the boat's heading and the actual heading is called the course. Since the boat often changes course, it moves along a curved trajectory; hence, the drift angle is the difference in direction between the course and the tangent to the path of the centre of gravity [9].

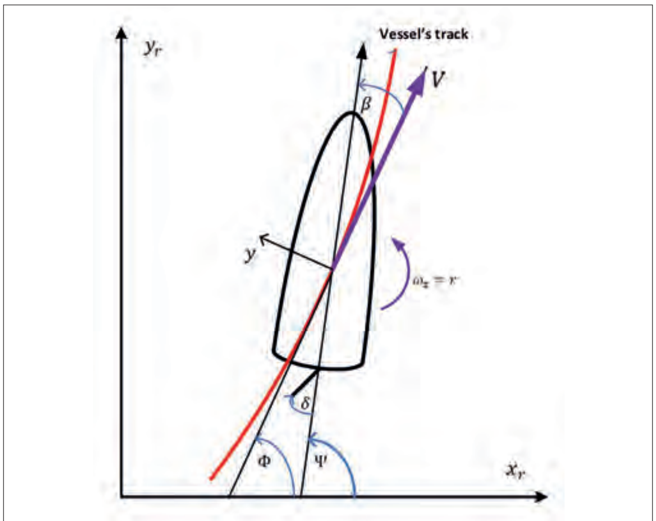

Fig. 2. Coordinate system and definition of the basic parameters f or 3DOF movement

Adopting a simplified system with 3DOF allows us to model the forces acting on the boat in the form of the drag, thrust and steering forces on the rudder. The equations are also supplemented with the transverse forces and moments on the hull. The main movement parameters are:

δ – rudder angle [deg]
β – drift angle ($\beta = \psi - \Phi$) [deg]
ψ – heading [deg]
Φ – course [deg]
r – rate of turn ($r = \omega_z = d\psi/dt$)

The equations for translation and rotation under 3DOF motion of a vessel are presented in Table 1.

Tab. 1. Translation and rotation for 3DOF motion of a vessel

Type of motion	Description	Equation
Translation	Surge	$u = V \cdot \cos\beta$
	Sway	$v = -V \cdot \sin\beta$
Rotation	Yaw	$r = d\Psi/dt$

For the initial analytical tests and to enable future validation of the model, the hull simulation model is created with 1DOF. The increase in the rotational speed of the propeller shaft is not proportional but depends on the characteristics of the PID controller.

The fundamental dynamics of manoeuvring and heading can be described using Newton's equations of motion. As an introduction to ship dynamics, a simplified equation of motion for ships with 1DOF, such as full-ahead-to-stop and emergency STOP, is given in Eq. (1).

$$m\,\frac{dV}{dt} = \sum F \tag{1}$$

For simplified 1DOF motion of a ship along a straight path, this equation represents the equilibrium of forces acting on the boat, i.e. the inertial forces due to the acceleration of the vessel, consisting of the weight of the boat and the added mass, multiplied by the acceleration due to the change in speed of the ship over time, and the equivalent force acting in the opposite direction, i.e. the thrust T of the propeller and the sum of the resistance forces of the boat R.

However, if the simulation model is to represent a 3DOF system, the system of forces will take the following form.

Longitudinal forces in the direction of the x-axis:

$$(m + m_x) \cdot \frac{dv_x}{dt} - (m - m_y) \cdot v_y \cdot \omega_z = F_x \tag{2}$$

Transverse forces in the direction of the y-axis:

$$(m + m_y) \cdot \frac{dv_y}{dt} - (m - m_x) \cdot v_x \cdot \omega_z = F_y \tag{3}$$

Rotating moment around the z-axis:

$$(I + I_z) \cdot \frac{d\omega_z}{dt} - (m_y - m_x) \cdot v_x \cdot v_y = M_z \tag{4}$$

where m_x, m_y are the added masses due to the inertia of the water when accelerating in the x- and y-directions, respectively.

In order to model an equation in MATLAB, it is necessary to arrange the terms in the so-called Cauchy form, where the first derivatives only appear on the left-hand side, i.e. [12]:

$$x' = f(x, t) \tag{5}$$

Hence, we have

$$v'_x = \frac{m+m_y}{m+m_x} \cdot v_y \cdot \omega_z + \frac{F_x}{m+m_x} \tag{6}$$

$$v'_y = -\frac{m+m_x}{m+m_y} \cdot v_x \cdot \omega_z + \frac{F_y}{m+m_y} \tag{7}$$

$$\omega'_z = \frac{M_z}{I+I_z} = r' \tag{8}$$

The formulae for the course and coordinates of the trajectory in this form are shown below.

$$\Psi' = \omega_z = r \tag{9}$$

$$x_r' = \sqrt{(v_x^2 + v_y^2)} \cdot \cos\phi \tag{10}$$

$$y_r' = \sqrt{(v_x^2 + v_y^2)} \cdot \sin\phi \tag{11}$$

$$\phi = \Psi - \beta \tag{12}$$

where

$$\beta = \arcsin\left(\frac{v_y}{V}\right) \tag{13}$$

$$v_y = -V \cdot \sin\beta \; for \; V = \sqrt{(v_x^2 + v_y^2)} \tag{14}$$

F_x – thrust force T,
F_y – steering force.

In the 1DOF simulation model, it is assumed that high-speed, round bilge displacement forms the hull. The method published by Marwood et al. in 1969 and by Bailey in 1976 was used to calculate the resistance [9][20].

The NPL round bilge high-speed hull series is over 40 years old, but is still well regarded as a drag prediction method for high-speed pilot or patrol boats. The graph used for calculation is presented in Fig. 3. It is designed to work over a range of Froude numbers F_{nL} = 0.3–1.2 ($F_{n\blacktriangledown}$ = 0.6–3.0). The method includes the following requirements:
– length to beam ratio L/B = 3.33–7.50,
– length to displacement ratio (M) = 4.5–8.3,
– beam inclination coefficient L/B = 1.75–10.77,
and constant values are assumed for:
– the position of the longitudinal centre of buoyancy L_{CB} = 6.4%L aft amidships,
– the block coefficient C_B = 0.397,
– the ratio of the transom area to maximum cross-sectional area A_T/A_X = 0.52 (where A_T is the transom area, and A_X is the maximum section area),
where
F_{nL} – Froude number $v/\sqrt{gL}$,
$F_{n\blacktriangledown}$ – volumetric Froude number $v/\sqrt{g\nabla^{1/3}}$,
M – $L/\nabla^{1/3}$.

The simulation model assumes that the resistance values are calculated from the measured resistance model by subtracting the frictional resistance, as determined using the 1957-ITTC skin friction formulation. The residuary resistance–displacement weight ratio uses the curve for $F_{n\blacktriangledown}$ = 1.1 [9].

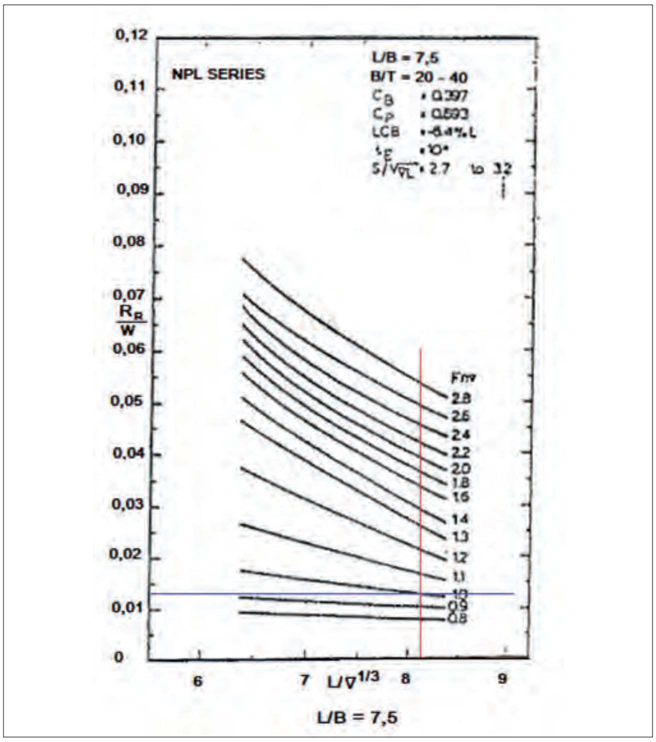

Fig. 3. Average values of the residual resistance–displacement weight R_R/W for the NPL methodical series with L/B=7.5 [9]

SHIP MOTION CONTROL SYSTEM

The propulsion engine (gas turbine engine) was taken as the control object in the automatic control system adopted here. Considering the gear ratio, the controlled variable is the shaft line's rotational speed, compared with the desired value in the summation node. The difference between these values is known as the control error, based on which the controller generates a control signal to reduce the value of this error. The control signal is then fed to the actuator, which determines the fuel flow rate to the propulsion engine. The flow rate affects the rotational speed of the shaft line, which is determined by the measuring system placed in the feedback loop. In turn, the rotational speed of the shaft line forms the input signal to the propeller block, where the forward speed and distance are calculated based on the hydrodynamic parameters of the unit and the propeller (see Fig. 4).

To implement the "Set value" module, the step block from the Simulink/Sources library was used. This block enables the execution of the step function at a defined point in time. For the simulation, a step change of the set value from zero to 15

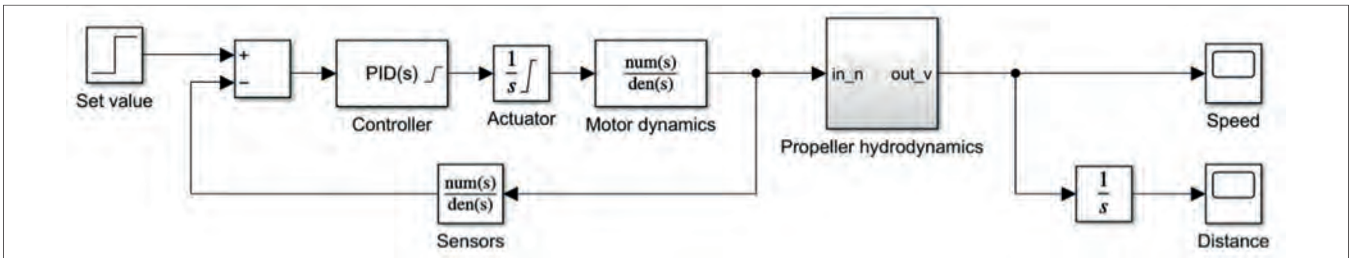

Fig. 4. Motion control system for a ship

(the rotational speed of the shaft line in rps) was assumed in the zero seconds of the simulation.

The use of a PID controller block is a classic approach to implementing a control system in which the control process can be improved by introducing proportional, derivative and integral coefficients. In this way, the controller ensures that the output is proportionate to the input signal and its derivative and integral. The solution adopted here assumes the implementation of a regulator with the following transfer function:

$$C_{par}(s) = P + I\left(\frac{1}{s}\right) + D\left(\frac{N_s}{s+N}\right), \tag{15}$$

for which the regulator settings are determined on the basis of two methods: the Ziegler-Nichols second method, and the Chien, Hrones and Reswick's step response method [22]. The settings obtained with both methods are presented in Table 2.

Tab. 2. PID controller settings

Parameter	Ziegler-Nichols method	Step response method
P	9.9	5.6
I	3.1	4.9
D	0.8	3.1

The designed control system gave similar performance for both settings, but the regulator tended to become highly saturated for the settings obtained using the step response method. Consequently, the settings acquired with the Ziegler-Nichols method were implemented, and an anti-windup system was incorporated into the PID block. The control output from the regulator obtained during the simulation of acceleration for a fast boat is depicted in Fig. 5.

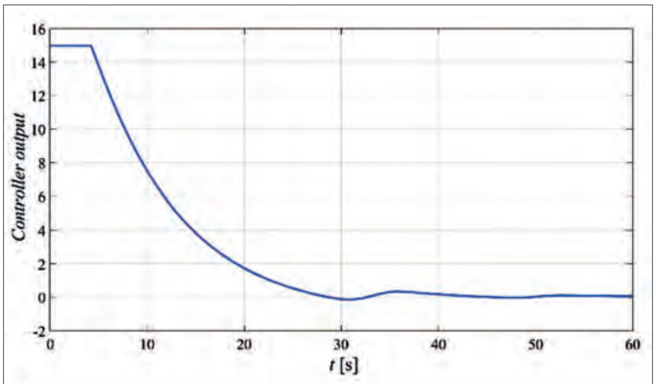

Fig. 5. Output of the controller during acceleration of a fast boat

The actuator usually consists of a DC electric motor and a gear train, and is modelled as an ideal integrating element, since if the inductance of the rotor winding and its moment of inertia are ignored, the armature supply voltage is proportional to the gear shaft's rotation angle. The "Integrator" block from the Simulink/Continuous library was adopted as the actuator module. This block defines the minimum and maximum values for signal saturation, which were set to zero and 15, respectively. These values correspond to the minimum and maximum fuel flow rate to the propulsion engine, respectively.

The propulsion engine was modelled as a second-order inertial term, described by the following operator transfer function:

$$G(s) = \frac{1}{10s^2 + 10s + 1} \tag{16}$$

The "Transfer Fcn" block from the Simulink/Continuous library was used to implement the simulation model. This block models linear systems using the Laplace transform.

The measuring system was modelled as a first-order inertial term with the following operator transfer function:

$$G(s) = \frac{1}{3s + 1} \tag{17}$$

In the simulation model, this was implemented using the "Transfer Fcn" block from the Simulink/Continuous library.

The "Propeller hydrodynamics" module contains a subsystem representing the hydrodynamic relationships for the vessel and the propeller. This module is an original solution proposed by the authors to bring the simulation results closer to the actual values obtained during sea trials. The equations used to describe the hull resistance, thrust force, and rudder forces have been supplemented in the text of the work. Air drag was omitted from the simulation model, as our research focused on the superstructure drag for a scale model. Due to the use of a hybrid model based on a MATLAB script (forces and moments) and Simulink (PID governor), the overall computational program and the structure of the propeller hydrodynamics block calculation algorithm are not presented here.

SIMULATION RESULTS

Using the coordinate system shown in Fig. 1, the acceleration of the boat was initially simulated only for 1DOF, representing surge. This check was carried out to verify the correct operation of the PID governor without interference from other DOF.

The object for the simulation models was a fast patrol boat with a length of L_{OA} = 34 m, a displacement of D = 74 m^3 and a maximum speed of v_{max} = 38 kt. A gas turbine was assumed to power the ship, with continuous power N = 4000, *shp* = 2983 kW. Simulation models were developed to compare the propulsion with two different types of propeller, a Wageningen B-series FPP propeller, four wings, AE/AO = 1.05, P/D = 1.4, and a Wageningen B-series propeller, five wings, AE/AO = 0.95, P/D = 1.3, with diameters of 1.32 and 1.3 m, respectively.

The thrust was calculated using the following formula:

$$T = K_T(J) \cdot \rho \cdot n^2 \cdot D^4 \tag{18}$$

where: n is the shaft rotation [rps], ρ is the density of sea water, D is the propeller diameter, and K_T is the thrust coefficient, which was introduced as a variable and is dependent on the value of J (the advance ratio), obtained by interpolation. The thrust coefficients vs advance coefficients approximation models gave values of R^2 > 0.99, indicating a good fit. Similar fitting results were obtained for the models of torque coefficients vs. advance coefficients.

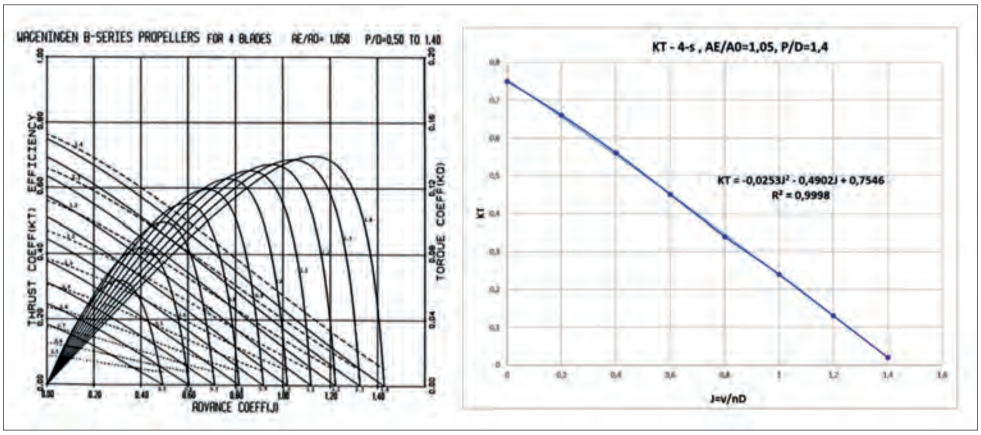

Fig. 6. Thrust coefficient for a four-blade propeller and its approximation model [21]

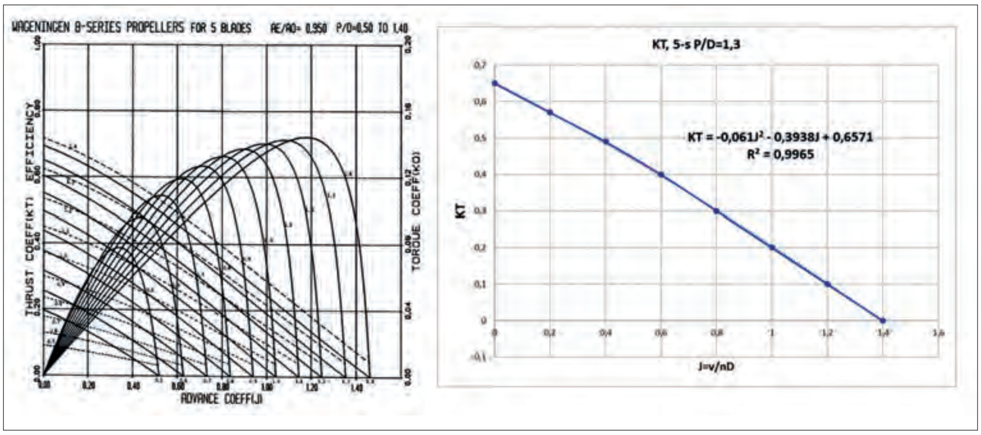

Fig. 7. Thrust coefficient for a five-blade propeller and its approximation model [21]

The fitting results for the two models in terms of K_T vs. J are presented in Figs. 6 and 7.

In the marine literature, numerous algorithms have been used to calculate the hydrodynamic forces on the rudder. In this work, we use the model of Inoue et al. [20] (see Fig. 2), where the rudder forces are defined as:

$$Y_R = |F_N \sin\delta|$$

$$X_R = a_x F_N \cos\delta$$

$$M_R = a_z F_N \cos\delta \tag{19}$$

where:

δ – rudder angle,

a_x – coefficient of influence of the hull over the force X_R on the rudder,

a_z – coefficient of influence of the hull over the moment M_R on the rudder, where

$$a_z = a_x \cdot y_R \tag{20}$$

y_R – distance of the rudder from the ship's centre of gravity G,

F_N – normal force on the rudder,

$$F_N = \frac{1}{2}\rho_w \frac{6.13 \cdot \lambda}{\lambda + 2.25} A_R V_R^2 \alpha_R \tag{21}$$

λ – aspect ratio of rudder,

A_R – rudder area,

V_R – velocity of water inflow to rudder,

α_R – effective angle of attack.

The simulation studies were divided into two stages. In the first stage, the sensitivity of the model with a PID controller was analysed for two FPPs, i.e. a four-blade and a five-blade propeller. The second stage of the research focused on a comparison of the simulation results using a PID controller and a model with a step increase in the shaft line speed. At this stage, the aims of the study were to identify differences in the dynamic parameters describing the movement of the boat and to assess the relative errors when using a simplified model without a PID governor for the engine [8].

The results of our analysis of the dynamics of the propellers indicate similar acceleration times (Fig. 8). However, an increase in ship speed is more effective for the five-blade propeller (Fig. 9). The use of a PID controller in the model means that the increase in the ship's speed is more consistent with the actual behaviour.

An analysis of the distance travelled also indicates a more effective use of the five-blade propeller (Fig. 10), which is confirmed by the difference in the thrust generated by the propellers (Fig. 11).

From Figs. 12 to 14, we can see that there are differences in:

- the dynamics of the propeller shaft with and without the PID governor,
- the distances travelled with and without the PID governor,
- the speed of the vessel with and without the PID governor.

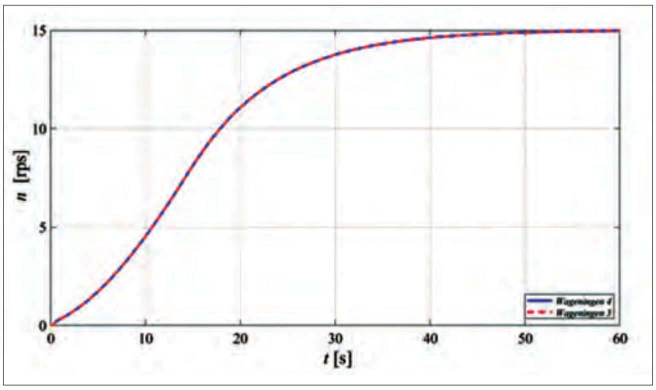

Fig. 8. Rotational speed of the shaft for two types of propeller

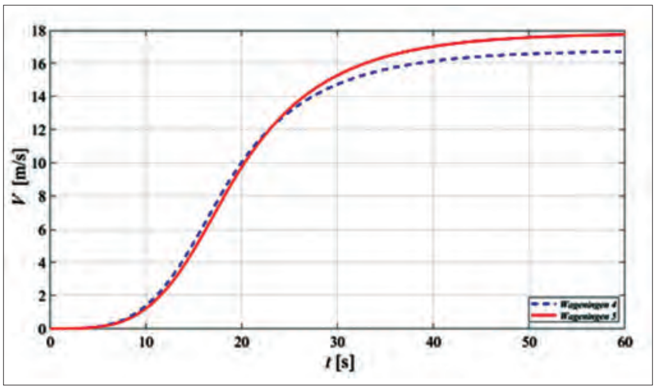

Fig. 9. Speed of the ship for two types of propeller

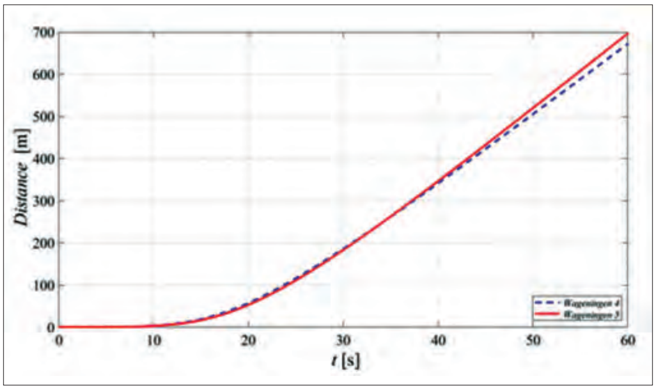

Fig. 10. Distance travelled for two types of propeller

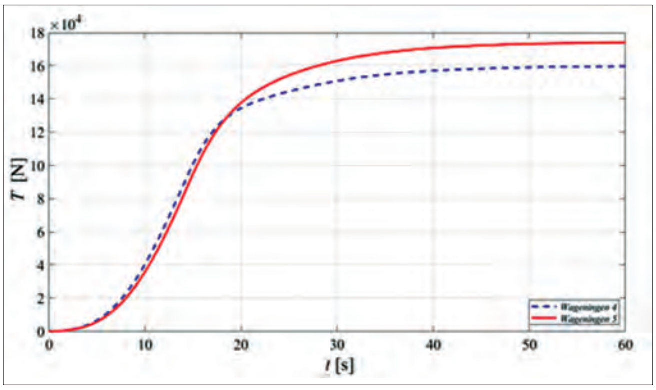

Fig. 11. Thrust generated by two types of propeller

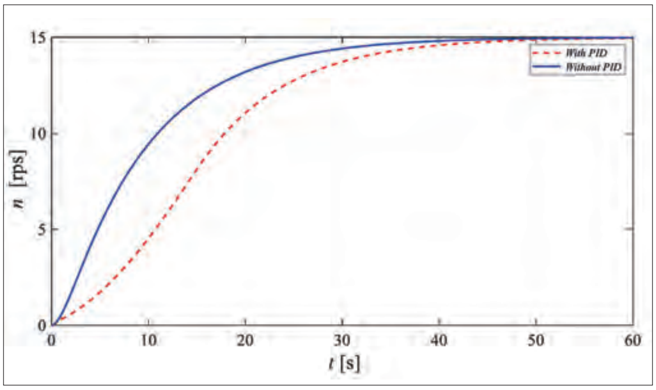

Fig. 12. Propeller's shaft dynamics with and without PID governor

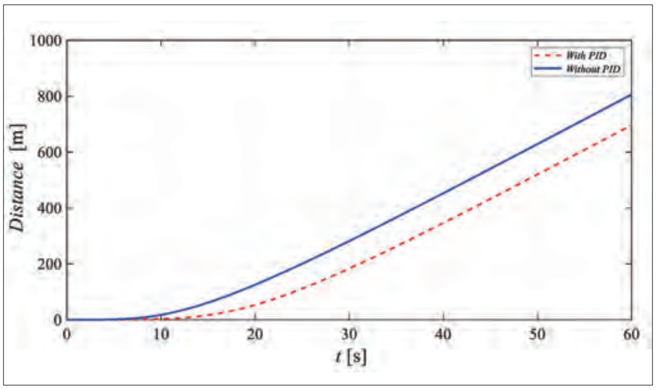

Fig. 13. Distances travelled with and without PID governor

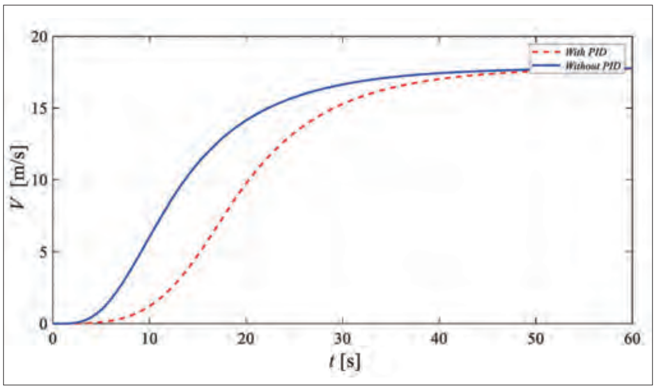

Fig. 14. Vessel's speed with and without PID governor

The introduction of the PID governor to the simulation model makes the increase in rotational speed more realistic and the time required to achieve the intended speed and distance longer. This model is significantly more accurate, and the results may substantially improve safety when planning experimental research.

CONCLUSION

The fundamental research problem addressed in this work was to demonstrate that the results of simulations of the acceleration of a fast boat without a PID governor on the engine may be significantly different from the results with a PID governor and from the results of validation tests during sea trials. The method of operation of the PID governor markedly affects the rotational acceleration of the propeller shaft and the acceleration of the boat. In addition, changes in the relationship between the boat's translational speed and the propeller's rotational speed change the instantaneous values of the thrust coefficient K_T, which also significantly affects the boat's acceleration time. Proper adjustment of the characteristics of the PID governor can solve these problems. A significant issue is the accurate matching of the characteristics of the governor; the potential error, even with differences in PID characteristics, will be smaller than if a linear acceleration of the propeller rotational speed is assumed in the simulation model. This issue is observed to be much less important during deceleration of the boat.

Planning sea trials is subject to restrictions regarding navigational safety. A knowledge of the time and distance involved when accelerating the vessel allows the researcher to prepare and carry out this task without the risk of collision, grounding, etc. A simulation model can greatly facilitate this process. Moreover, a well-prepared open-type model allows for changes in input parameters and analysis for different types of boats.

We carried out a comparative analysis of the models with and without a PID controller, in terms of:

- the propeller acceleration time,
- the time required to reach the maximum speed,
- the distance travelled before reaching the maximum speed.

The proposed simulation model shows significant differences in the dynamics of the propeller shaft, and the use of a PID governor can correct these simulation results to be more similar to those under real conditions. The settings for the governor were determined using two methods: the Ziegler-Nichols second method, and the Chien, Hrones and Reswick's step response method. Since the governor tended to become highly saturated under the settings obtained using the step response method, the settings acquired with the Ziegler-Nichols method were deployed in the simulation, and an anti-windup system was incorporated into the PID block.

Air drag was omitted from the simulation model due to a lack of data enabling the calculation of the air drag coefficient, C_A. With our next model, we will analyse the impact of the shape of the boat superstructure on C_A, the impact of a virtually introduced wind from directions between 0° and 360° in steps of 10°, and the impact of changes in wind speed from 2 to 20 m/s in steps of 2 m/s.

REFERENCES

1. T. H. Le *et al.*, "Numerical investigation on the effect of trim on ship resistance by RANSE method," *Applied Ocean Research*, vol. 111, 2021, doi: 10.1016/j.apor.2021.102642.

2. S. Song, M. Terziev, T. Tezdogan, Y. K. Demirel, C. De Marco Muscat-Fenech, and A. Incecik, "Investigating roughness effects on ship resistance in shallow waters," *Ocean Engineering*, vol. 270, 2023, doi: 10.1016/j.oceaneng.2023.113643.

3. C. G. Källström and K. J. Åström, "Experiences of system identification applied to ship steering," *Automatica*, vol. 17, no. 1, 1981, doi: 10.1016/0005-1098(81)90094-7.

4. T. Perez, A. Ross, and T. Fossen, "A 4-DOF simulink model of a coastal patrol vessel for manoeuvring in waves," in *Proceedings of the 7th IFAC Conference on Manoeuvring and Control of Marine Craft*, 2006.

5. A. Dogrul, S. Song, and Y. K. Demirel, "Scale effect on ship resistance components and form factor," *Ocean Engineering*, vol. 209, 2020, doi: 10.1016/j.oceaneng.2020.107428.

6. S. Sutulo and C. Guedes Soares, "On the application of empiric methods for prediction of ship manoeuvring properties and associated uncertainties," *Ocean Engineering*, vol. 186, 2019, doi: 10.1016/j.oceaneng.2019.106111.

7. S. Tavakoli, S. Najafi, E. Amini, and A. Dashtimansh, "Ship acceleration motion under the action of a propulsion system: a combined empirical method for simulation and optimisation," *Journal of Marine Engineering and Technology*, vol. 20, no. 3, 2021, doi: 10.1080/20464177.2020.1827490.

8. Z. Świder, L. Trybus, and A. Stec, "Consistent Design of PID Controllers for an Autopilot," *Polish Maritime Research*, vol. 30, no. 1, 2023, doi: 10.2478/pomr-2023-0008.

9. E. V. (ed.) Lewis, *Principles of naval architecture. 2nd reversion, vol IlL Motions in waves and controllability*, vol. 3. 1989.

10. A. Stotsky and A. Forgo, "Recursive spline interpolation method for real time engine control applications," *Control Eng Pract*, vol. 12, no. 4, 2004, doi: 10.1016/S0967-0661(03)00114-X.

11. S. M. Sajedi and P. Ghadimi, "Experimental and Numerical Investigation of Stepped Planing Hulls in Finding an Optimized Step Location and Analysis of Its Porpoising Phenomenon," *Math Probl Eng*, vol. 2020, 2020, doi: 10.1155/2020/3580491.

12. "Some Other Classes of Numerical Methods," in *Partial Differential Equations with Numerical Methods*, 2008. doi: 10.1007/978-3-540-88706-5_14.

13. A. Esfandiari, A. Hosseini Monjezi, M. Rezakazemi, and M. Younas, "Computational fluid dynamic modeling of water desalination using low-energy continuous direct contact membrane distillation process," *Appl Therm Eng*, vol. 163, 2019, doi: 10.1016/j.applthermaleng.2019.114391.

14. L. Birk, "Holtrop and Mennen's Method," in *Fundamentals of Ship Hydrodynamics*, 2019. doi: 10.1002/9781119191575.ch50.

15. Z. Dong, J. Li, W. Liu, H. Zhang, S. Qi, and Z. Zhang, "Adptive Heading Control of Underactuated Unmanned Surface Vehicle Based on Improved Backpropagation Neural Network," *Polish Maritime Research*, vol. 30, no. 1, 2023, doi: 10.2478/pomr-2023-0006.

16. T. C. My, L. D. Khanh, and P. M. Thao, “An Artificial Neural Networks (ANN) Approach for 3 Degrees of Freedom Motion Controlling,” *International Journal on Informatics Visualization*, vol. 7, no. 2, 2023, doi: 10.30630/joiv.7.2.1817.

17. J. Yang, J. Feng, Y. Li, A. Liu, J. Hu, and Z. Ma, “Water-exit process modeling and added-mass calculation of the submarine-launched missile,” *Polish Maritime Research*, vol. 24, no. S3, 2017, doi: 10.1515/pomr-2017-0118.

18. P. A. Wilson, “A review of the methods of calculation of added resistance for ships in a seaway,” *Journal of Wind Engineering and Industrial Aerodynamics*, vol. 20, no. 1–3, 1985, doi: 10.1016/0167-6105(85)90018-2.

19. S. Song et al., “Experimental investigation on the effect of heterogeneous hull roughness on ship resistance,” *Ocean Engineering*, vol. 223, 2021, doi: 10.1016/j.oceaneng.2021.108590.

20. D. Bailey, “The NPL Round Bilge Displacement Hull Series,” *Maritime Technology Monograph No. 4. Royal Institution of Naval Architectcs*. 1976.

21. M. M. Bernitsas, D. Ray, and P. Kinley, “KT, KQ and efficiency curves for the wageningen b-series propellers,” *237*. 1981.